

RESEARCH ARTICLE

 OPEN ACCESS

Received: 03-12-2022

Accepted: 13-02-2023

Published: 27-03-2023

Citation: Murthuza KM, Surumbarkuzhali N, Lakshmi Narasimhan C, Ravisankar R (2023) Using Magnetic Susceptibility to Assess Soil Pollution in the Tiruvannamalai District, Tamil Nadu with Statistical Approach. Indian Journal of Science and Technology 16(12): 910-923. <https://doi.org/10.17485/IJST/v16i12.2326>

* **Corresponding author.**muthuza@gmail.com**Funding:** None**Competing Interests:** None

Copyright: © 2023 Murthuza et al. This is an open access article distributed under the terms of the [Creative Commons Attribution License](https://creativecommons.org/licenses/by/4.0/), which permits unrestricted use, distribution, and reproduction in any medium, provided the original author and source are credited.

Published By Indian Society for Education and Environment ([iSee](https://www.isee.org/))

ISSN

Print: 0974-6846

Electronic: 0974-5645

Using Magnetic Susceptibility to Assess Soil Pollution in the Tiruvannamalai District, Tamil Nadu with Statistical Approach

K Mohammed Murthuza^{1*}, N Surumbarkuzhali¹, C Lakshmi Narasimhan², R Ravisankar³

¹ Post Graduate and Research Department of Physics, Government Arts College, Salem, 636007, Tamil Nadu, India

² Department of Geology, Anna University, Kotturpuram, Chennai, 600025, Tamil Nadu, India

³ Post Graduate and Research Department of Physics, Kalaignar Karunadhi Government Arts College, Tiruvannamalai, 606603, Tamil Nadu, India

Abstract

Objective: This study used magnetic susceptibility measurements and statistical methods to investigate soil pollution. **Method:** Using the grid approach, soil samples were collected in and around Tiruvannamalai district, Tamil Nadu. Standard procedures were used to determine the physicochemical parameters of soil samples such as the percentages of sand, silt and clay, EC and pH. A dual frequency susceptibility meter was used to assess the magnetic susceptibility of the soil samples collected at low-frequency (χ_{lf}) and high-frequency (χ_{hf}). Multivariate statistical analysis such as factor analysis (FA), Pearson correlation (PC), and cluster analysis (CA) were conducted to determine the influence of Physicochemical parameters on magnetic susceptibilities and to detect soil contamination from anthropogenic or natural sources. **Findings:** Significant magnetic enhancement values may be concentrated in the soil, indicating ferrimagnetic minerals in the study area in some locations. **Novelty:** Contamination sources of pollution using magnetic susceptibility with statistical approach.

Keywords: Soil; Physicochemical properties; magnetic susceptibility; Statistical Methods; Pollution

1 Introduction

Our environment is composed of four elements: (i) Atmosphere, (ii) Earth (iii) Water, and (iv) Space. It remains clean and enjoyable in the absence of pollution. However, as a result of man's multiple activities, the Environment becomes polluted, which is referred to as Environmental pollution. Environmental pollution is one of the most serious future threats to the society. Rapid population growth is one of the primary causes of environmental degradation in developing countries, putting natural resources and the environment at risk.

Soil contamination occurs as a result of the disposal of plastics, textiles, glass, metal, and organic matter, as well as sewage, sewage sludge, and building debris produced

by residences, business complexes, and factories. Soil pollution is caused by on-land disposal of fly ash, iron and steel slag, medical and industrial wastes. Agricultural fertilizers and pesticides that infiltrate the soil through run-off and land filling with city garbage are becoming a bigger problem. Soil pollution is also exacerbated by acid rain and pollutant deposition on the ground surface.

Numerous studies have found that the magnetic properties of anthropogenic particles may contain information about their origins and can therefore be used to detect their source of emission⁽¹⁻⁴⁾. The exact sources of pollution have been successfully identified using magnetic measurements^(5,6). Magnetic susceptibility is a mineralogical covariate measure; thus, its changes can be interpreted as a soil's magnetic signature, which is sensitive to mineral types and characteristics, as well as the formation environment (genesis). According to Maher and Thompson⁽⁷⁾, the factors and processes that contribute to soil formation can be recorded using magnetic minerals. These minerals exhibit four unique magnetic properties and occur naturally in mineral soils: ferromagnetic (for example, magnetite, maghemite, and ferromagnetic ferridryte), antiferromagnetic (for example, hematite and goethite), diamagnetic (for example, quartz), and paramagnetic (for example, olivine)⁽⁸⁾. Magnetic susceptibility has been extensively used in environmental and soil sciences as a proxy for the presence of ferrimagnetic minerals (predominantly magnetite and maghemite) in soils⁽⁹⁾. With this context in mind, this study investigated the possibility of using magnetic susceptibility to distinguish between sources of soil pollution.

The objective of this research is i) to establish direct evidence that magnetic properties can be used to determine the degree of soil contamination. ii) to identify the sources of soil pollution iii) to determine the effectiveness of magnetic susceptibility and iv) to use statistical approaches to analyze the correlations between soil parameters and magnetic susceptibility.

2 Materials and Methods

2.1 Sample collection and preparation

This research is being conducted in the district of Tiruvannamalai, which spans an area of 6188 km² and is located at 11.55° and 13.15° North Latitude and 78.20° and 79.50° East Longitude (Figure 1). Soil samples were collected using the grid method in the Tiruvannamalai district of Tamilnadu⁽¹⁰⁾. The district's land cover is depicted in the Figure 2 as square grids (10.85 km x 10.85 km) using QGIS – open source mapping software. Each grid was assigned a location (W1-W63 as mentioned in Figure 2) based on the availability and approachability of the sampling site⁽¹⁰⁾. The samples were collected from the grid node points of the square grid. To collect the sample, a 1m X 1m undisturbed sampling sites were selected to ensure that the samples were not influenced by human made or anthropogenic activities. Four samples were collected in the corners of the square, and one sample was collected at the centre point⁽¹¹⁾. These samples are mixed together to get representative samples. A bulk sample of 1kg was obtained, which had been air-dried, and larger stone fragments or shells had been handpicked. The samples were ground to a fine powder with an agate motor and stored in desiccators until analysed.

2.2 Determination of Physicochemical properties

The soil characteristics such percentage of sand, silt, and clay were determined using the Mechanical sieve shaker method which is extremely effective⁽¹²⁾. In ascending order, a sieve shaker with sieves of various sizes (12 mm, 150 mm, and 200 mm) was set up. A weighed sample is delivered to the top sieve, which has the largest screen openings. The gaps in the column's lower sieves are smaller than those in the upper sieve. The receiver is a round pan at the base of the column. A mechanical shaker is typically used to position the column and shakes it up. The sample in each sieve is weighed after the shaking is finished. The percentages of sand, slit, and clay in samples are then calculated using the following equation:

$$\text{Soil characteristics (\%)} = \frac{W1}{W2} \times 100 \quad (1)$$

W1 is the weight of the sample retained in each sieve, and W2 denotes the total weight of the sample used for the tests. A pH measuring potentiometer is used to determine the acidity or alkalinity of the suspended water samples and the 0.01 M calcium chloride solution. Prior to sample analysis, the potentiometer is calibrated with buffer solutions of known pH values. The electric conductivity was measured using a digital conductivity meter. The reference solution used is a 0.005 N KCl solution with an electrical conductivity of 720±1 dS/m at 25°C⁽¹³⁾. The Electrical Conductivity is measured in decisiemens per metre. A 25-gram sample is mixed in 40-milliliters of deionized water, yielding a water/soil ratio of 2:1. The conductivity of the sample was determined by inserting an electrode into the solution.

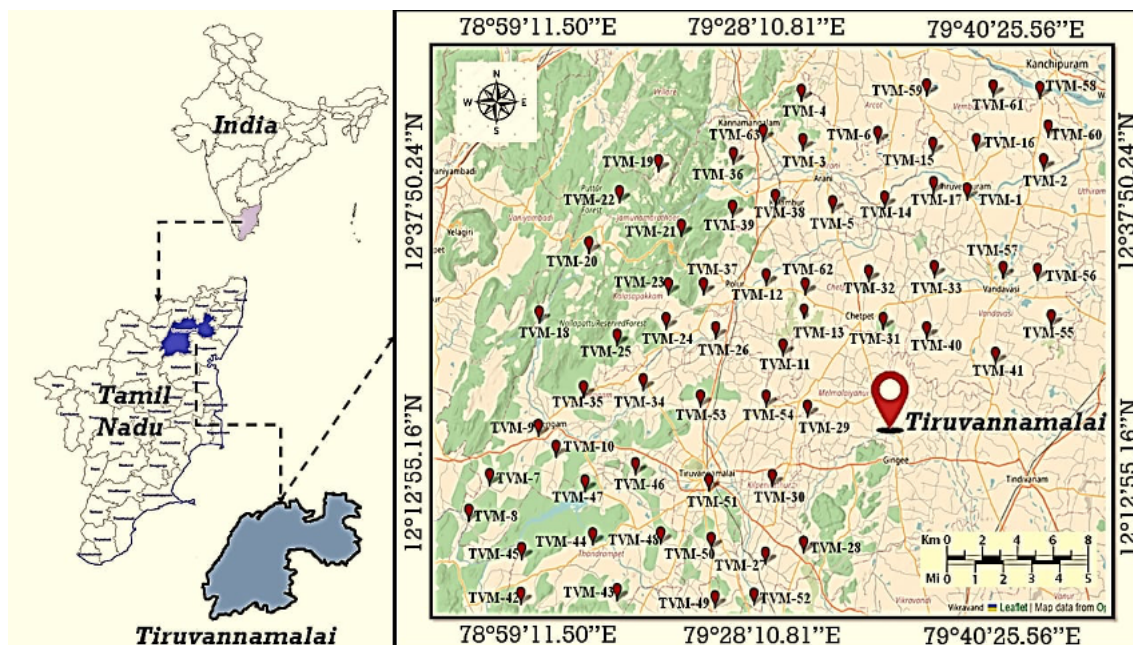


Fig 1. Location of the study area - Tiruvannamalai District

Sampling sites - with GPS Coordinates (GRID sampling)

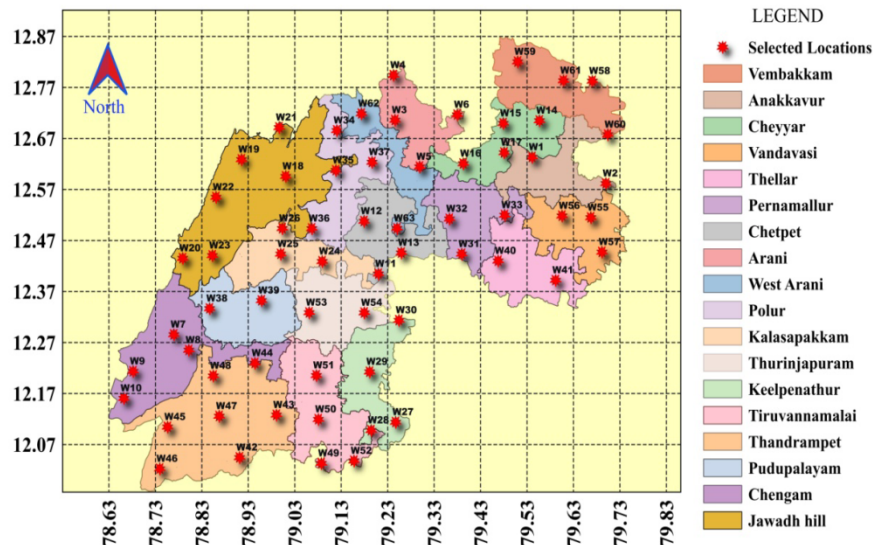


Fig 2. Sampling Sites with GPS Coordinates within the grids

2.3 Magnetic susceptibility (χ) measurements

The excess water in the samples was air dried in the laboratory at room temperature to prevent any chemical reactions. The samples were then sieved through a 1 mm mesh to remove glass, plant waste, refuse, and small stones⁽¹⁴⁾. The sieved samples were then transferred to a plastic container and transported to the laboratory for further analysis. Magnetic susceptibility measurements were performed on sieved samples packaged in a 10 ml plastic container at laboratory temperature at low (0.465 kHz) and high (4.65 kHz) frequencies using an MS2B dual frequency susceptibility meter connected to a computer operating in Multisus2 software. The sensitivity setting was set to 1.0 for all measurements. Each sample was tested for five times at two distinct frequencies (low and high), and an average was computed. It can be used as a proxy for the relative concentration changes in pedogenic fine-grained magnetic particles in natural samples with a continuous and nearly constant grain size distribution⁽¹⁵⁾. As a result, the expression for frequency dependent susceptibility (fd) was used⁽¹⁶⁾.

$$\chi_{fd}(\%) = \left[\frac{(\chi_{lf} - \chi_{hf})}{\chi_{lf}} \right] \times 100 \tag{2}$$

2.4 Multivariate statistical analysis

The multivariate statistical analyses such as Pearson correlation, factor and cluster analysis were done for the better understanding of the relationship between physico-chemical properties and magnetic susceptibility in soil samples. This relationship was used to divide pollution into two categories: natural and man-made. The statistical analysis was carried out with the help of the statistical software SPSS (Statistical Package for Social Science16.0 version).

3 Results and Discussion

3.1 Sand, Silt and Clay Analysis

The sand, silt, clay, and physico-chemical properties are shown in Table 1. The sand percentages range from 61% to 90%, with an average of 76.46% across all locations. In comparison to Silt and Clay, Sand is the most common constituent in all sampling locations in the research area.

Table 1. Physico-chemical properties and Magnetic susceptibilities in soils of Tiruvannamalai district, Tamil Nadu

S.No	Sample ID	Location Name	Latitude	Longitude	Physico-chemical Properties					Magnetic susceptibilities		
					Sand %	Slit %	Clay %	Conductivity (MS)	pH	LF*	HF*	%FD
1	TVM 1	Anakkavaur	12°38'06.08"	79°32'38.21"	65	21	14	137	6.19	382.56	381.2	0.36
2	TVM 2	Vengodu	12°35'00.50"	79°42'10.59"	64	24	12	139	7.88	26.2	25.23	3.7
3	TVM 3	Agarapalayam	12°42'27.55"	79°14'56.16"	72	17	11	105.6	7.03	103.34	102.12	1.18
4	TVM 4	poosimalaikuppam	12°46'44.40"	79°14'44.14"	70	20	10	123	5.8	279.23	274.12	1.83
5	TVM 5	Pudhupattu	12°36'58.39"	79°18'06.66"	61	23	16	96.3	7.11	35.12	34.12	2.85
6	TVM 6	Randamkorrattar	12°43'5.54"	79°22'58.46"	80	13	7	120	7.92	392.54	391.76	0.2
7	TVM 7	Naradapattu	12°12'54.58"	78°41'06.25"	78	12	10	262	6.13	225.56	224.34	0.54
8	TVM 8	Neepathurai	12°09'44.33"	78°38'54.47"	76	15	9	137	5.5	84.32	82.34	2.35
9	TVM 9	Pakkaripalayam	12°17'14.34"	78°46'22.11"	82	11	7	119	6.2	309.53	307.27	0.73
10	TVM 10	Pinjur	12°15'24.41"	78°48'18.19"	73	18	9	130.5	7.16	1410.25	1405.87	0.31
11	TVM 11	Mansurabath	12°24'22.63"	79°12'47.32"	76	14	10	160	6.15	368.23	367.98	0.07
12	TVM 12	Pulivandal	12°30'34.38"	79°10'55.91"	64	21	15	228	6.16	60.24	59.45	1.31
13	TVM 13	Seyanandal	12°27'51.21"	79°15'44.90"	77	15	8	160.4	8.01	108.67	107.45	1.12
14	TVM 14	Devanathur	12°37'20.69"	79°23'45.15"	80	12	8	148	7.8	480.45	477.56	0.6
15	TVM 15	Murugathanpoondi	12°42'04.94"	79°28'54.94"	79	14	7	136	7.13	303.24	301.56	0.55
16	TVM 16	Nadumbarai	12°42'24.21"	79°33'35.34"	75	16	9	125	7.99	30.65	30.56	0.29
17	TVM 17	Parasur	12°38'38.17"	79°29'02.15"	80	11	9	69.5	6.07	170.9	169.89	0.59
18	TVM 18	Kilayur	12°27'12.75"	78°46'30.53"	80	13	7	159.2	7.6	70.23	67.54	3.83
19	TVM 19	Nammiyambattu	12°40'35.59"	78°59'18.00"	77	18	5	412	6.06	133.89	130.24	2.73
20	TVM 20	Palamarthur	12°33'23.55"	78°51'49.09"	75	14	11	163.2	7.91	46.65	46.12	1.14

Continued on next page

Table 1 continued

21	TVM 21	Seangadi	12°34'50.91"	79°01'49.07"	90	8	2	252	6.22	197.45	196.67	0.4
22	TVM 22	Veerappanur	12°37'49.55"	78°55'06.46"	64	24	12	144	6.32	99.8	99.67	0.13
23	TVM 23	Kidampalayam	12°29'43.40"	79°00'22.51"	70	19	11	201	6.08	165.32	165.78	0.92
24	TVM 24	Parvathimalai	12°26'42.89"	79°00'10.33"	81	12	7	120	6.25	253.23	252.78	0.18
25	TVM 25	Parvathimalai RF	12°25'14.23"	78°54'55.38"	82	11	7	120	6.29	1151.23	1142.45	0.76
26	TVM 26	Pillur	12°25'50.55"	79°05'31.78"	85	10	5	103.3	6.97	297.45	294.45	1.01
27	TVM 27	Angunam	12°05'58.21"	79°10'50.79"	90	7	3	123.8	7.04	649.1	645.34	0.58
28	TVM 28	Panniyur	12°06'56.14"	79°15'00.80"	88	8	4	679	6.34	394.67	393.54	0.29
29	TVM 29	Sevarapundi	12°18'55.10"	79°15'26.54"	89	9	2	118.1	7.3	432.76	415.56	3.97
30	TVM 30	Vedanatham	12°12'51.31"	79°11'39.18"	69	21	10	132.8	7.09	80.23	79.12	1.38
31	TVM 31	Melnanthiyambadi	12°26'42.64"	79°23'32.77"	81	11	8	137	6.75	54.45	52.12	4.28
32	TVM 32	Melpoondi	12°30'50.70"	79°21'57.89"	82	14	4	212	6.27	211.56	210.9	0.31
33	TVM 33	Vallam	12°31'16.88"	79°29'05.69"	86	9	5	72.4	6.75	1173.56	1171.23	0.2
34	TVM 34	Kanji	12°21'14.60"	78°57'41.36"	65	20	15	118	6.2	101.12	98.56	2.53
35	TVM 35	Monnormangalam	12°20'39.79"	78°51'13.91"	88	9	3	233	6.3	24.13	24.08	0.21
36	TVM 36	Ananthapuram	12°41'14.54"	79°07'25.22"	66	22	12	97.8	6.42	109.14	108.67	0.43
37	TVM 37	Edaipirai	12°29'42.32"	79°04'11.39"	88	9	3	89.3	7.06	58.45	57.65	1.37
38	TVM 38	Illupakkam	12°37'30.87"	79°11'58.18"	68	20	12	112	6.32	1664.9	1648	1.02
39	TVM 39	Thurinjikuppam	12°36'32.79"	79°07'17.97"	73	17	10	140	6.18	35.67	34.34	3.73
40	TVM 40	Seeyamangalam	12°25'54.09"	79°28'15.03"	88	8	4	152	8.13	69.89	67.78	3.02
41	TVM 41	Theyyar	12°23'37.51"	79°35'40.43"	65	21	14	144	7.75	23.25	22.76	2.11
42	TVM 42	Beemarapati	12°02' 27.18"	78°44'32.70"	72	17	11	118	6.12	921.78	905.89	1.72
43	TVM 43	Kuvilam	12°02'46.38"	78°54'51.39"	85	12	3	94.3	8.61	83.89	80.89	3.58
44	TVM 44	Malamanjanur	12°07' 38.58"	78°52'13.71"	71	19	10	131	6.15	162.67	161.76	0.56
45	TVM 45	Melpasar	12°06' 22.15"	78°44'33.54"	64	20	16	117.1	7.32	39.67	35.65	10.13
46	TVM 46	Nedungavadi	12°13'52.46"	78°56'50.23"	61	27	12	61.3	6.68	52.78	49.43	6.35
47	TVM 47	Sathanoor	12°12' 22.88"	78°51'27.46"	70	20	10	109.2	8.76	56.89	52.5	7.72
48	TVM 48	Vakkilpattu	12°07'46.85"	78°59'37.26"	81	12	7	712.04	6.45	23.5	22.34	4.94
49	TVM 49	Devanur	12°02'05.48"	79°05'25.13"	80	12	8	112.1	7.47	39.12	36.76	6.03
50	TVM 50	Kattampoondi	12°07'16.08"	79°05'02.03"	81	15	4	78.5	7.86	25.78	20.09	22.07
51	TVM 51	Melathikam	12°12'25.79"	79°04'46.54"	69	20	11	709	6.26	166.12	164.43	1.02
52	TVM 52	Virthuvilanginan	12°02'23.12"	79°09'38.20"	65	22	13	122	6.12	480.67	477.41	0.68
53	TVM 53	Karunthuvambadi	12°19'49.27"	79°03'50.62"	75	16	9	83.9	7	32.56	32.45	0.34
54	TVM 54	Mangalam	12°19'48.33"	79°10'57.77"	87	9	4	282	7.89	99.9	95.45	4.45
55	TVM 55	Badhur	12°26'56.57"	79°41'39.92"	88	10	2	113.2	6.41	569.76	568.12	0.29
56	TVM 56	Vazhur	12°30'59.93"	79°40'13.52"	72	18	10	108.8	7.55	85.12	82.34	3.27
57	TVM 57	Vengunam	12°31'12.10"	79°36'30.36"	86	11	3	83.7	6.87	63.34	61.01	3.68
58	TVM 58	Abdullapuram	12°47'03.42"	79°40'25.24"	69	19	12	108.5	7.42	37.23	36.78	1.21
59	TVM 59	Randam	12°47'15.45"	79°28'13.28"	84	10	6	743	7.56	457.09	453.78	0.72
60	TVM 60	Sodiambakkam	12°43'39.32"	79°41'22.92"	69	20	11	71	6.6	410.89	402.1	2.14
61	TVM 61	Vembakkam	12°47'12.71"	79°35'27.77"	80	12	8	92.3	6.84	523.76	518.76	0.95
62	TVM 62	Devikapuram	12°29'43.73"	79°15'11.49"	79	15	6	413.01	7.22	475.08	473.67	0.3
63	TVM 63	Ramasanikuppam	12°43'13.15"	79°10'35.56"	87	8	5	94.5	6.06	146.56	142.09	3.05
Minimum					61	7	2	61.3	5.5	23.25	20.09	0.07
Maximum					90	27	16	743	8.76	1664.9	1648	22.07
Average					76.46	15.15	8.38	177.62	6.873	273.38	270.50	2.227

Sand in Seangadi (TVM 21) indicates high quartz content, whereas the low percentage of sand in Nedungavadi (TVM 46) suggests that the studied area has a low light mineral content⁽⁶⁾. The silt concentrations range from 7% to 27%, with an average of 15.15 percent. The presence of primary minerals may account for the high percentage of slit in Nedungavadi (TVM 46)⁽¹⁷⁾. The concentration of clay ranges from 2% to 16%, with an average of 8.38%. Organic carbon may be present in Pudhupattu (TVM 5) due to its high clay composition. Pudhupattu (TVM 5) has a high clay concentration, indicating that the soil samples have higher organic carbon content.

3.2 PH

Table 1 shows the pH values of the soil samples studied. Many factors, including the organic composition of the soil, influence soil pH, which has a direct impact on plant growth. Soil samples had pH values ranging from 5.5 to 8.76, with an average of 6.873. Neepathurai (TVM 8) and Sathanoor (TVM 47) have the lowest and highest pH values, respectively. Certain locations in the study area had the lowest pH values, which could be related to microbial activity. High pH values noticed in some locations may be influenced by the calcareous parent materials, low rainfall and low forest density. Figure 3 shows the pH values of the samples and sample locations in the study area.

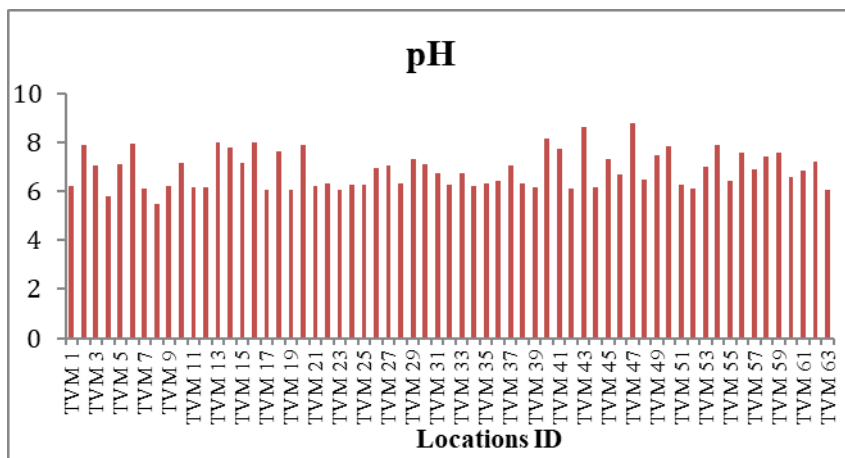


Fig 3. Location ID and pH of the samples

3.3 Electrical Conductivity (EC)

Electrical conductivity (EC) values in the soil samples ranged from 61.3 to 743 S/cm, with an average value of 177.62. In the study area, soil samples from Nedungavadi (TVM 46) and Ransom (TVM 59) were found to have low and high EC values, respectively. An increase in the EC value may be due to the effluent introducing a large amount of dissolved salts to certain soil locations. All of the soil samples had electrical conductivities ranging from 0 to 20000 S/m, indicating that the soil is suitable for plant growth. Figure 4 shows the conductivity values of the samples and locations in the study area.

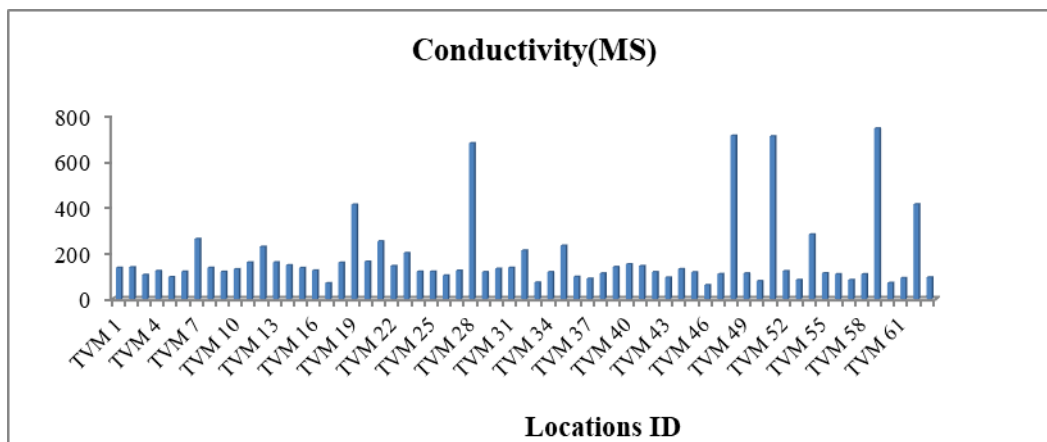


Fig 4. Location ID and Conductivity values of the samples

3.4 Magnetic susceptibilities in soils

Table 1 displays the magnetic susceptibility values of soil samples collected in the study area. The low frequency magnetic susceptibility ranges from $23.25 \times 10^{-5} \text{ m}^3 \text{ kg}^{-1}$ to $1664.9 \times 10^{-5} \text{ m}^3 \text{ kg}^{-1}$, with an average value of $273.38 \times 10^{-5} \text{ m}^3 \text{ kg}^{-1}$. As seen in Table 1, all soil samples χ_{lf} exhibits greater values than χ_{hf} . This disparity is caused by the presence of fine-grained superparamagnetic grains with relaxation durations shorter than the measurement time, which are magnetically blocked and hence do not contribute to the recorded signal⁽¹⁸⁾. Magnetic susceptibility variations are caused by a variety of factors, including lithological and geological variations (lithogenic/geogenic), soil formation processes (pedogenesis), and anthropogenic magnetic material contribution⁽¹⁹⁾. Figures 5 and 6 shows the variations of low frequency and high frequency magnetic susceptibility with the locations.

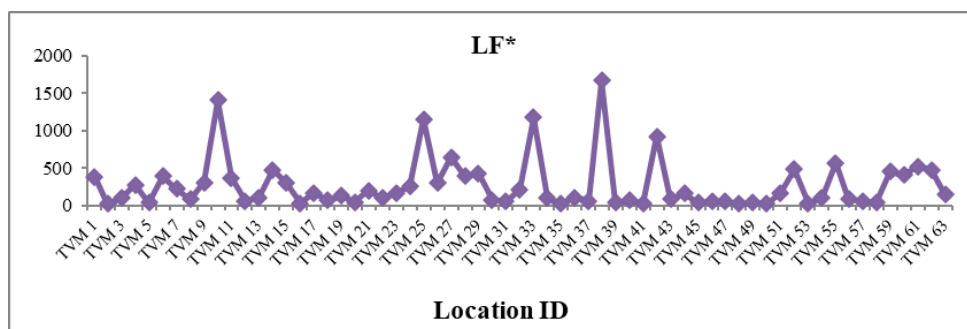


Fig 5. Location Vs Low Frequency Susceptibility (LF)($10^{-8} \text{ m}^3/\text{kg}$)

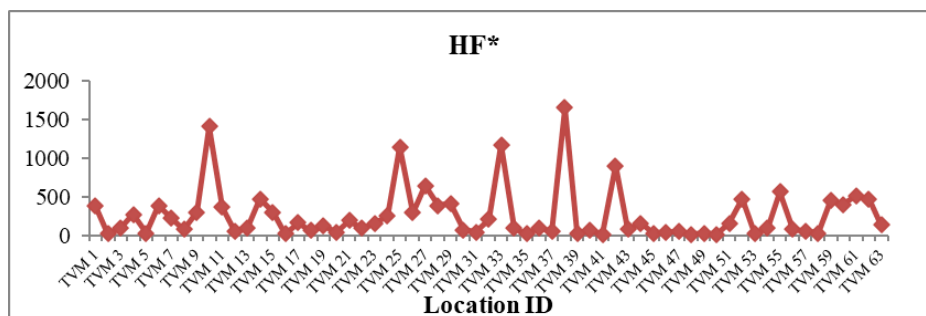


Fig 6. Location Vs High Frequency Susceptibility (HF)($10^{-8} \text{ m}^3/\text{kg}$)

Saddiki⁽²⁰⁾ confirmed that the primary factor affecting magnetic susceptibility variation is lithology. In some locations (TVM 10, TVM 25, TVM 33, TVM 38, TVM 41), the significant magnetic enhancement values indicate that the soil contains a high concentration of ferromagnetic minerals, possibly of pedogenic origin. The Fe^{2+} oxidation in iron-bearing minerals formed the Pedogenic ferrimagnetic minerals in soils subjected to wetting-drying cycles typical of the regional climate⁽²¹⁾. Furthermore, human-induced magnetic material inputs have resulted in an increase in soil magnetic enhancement. Magnetic particles that are anthropogenic are likely to come from vehicle emissions (exhaust, absorption). This may be related to the fact that automotive exhaust pipes produce a wide range of particle fractions, which are then released into the atmosphere. Magnetic measurements have shown that pollution in the soil can be detected using the results of this analysis.

3.5 Frequency dependent susceptibility

The relative loss of susceptibility (χ_{fd}) represents the difference between χ_{lf} and χ_{hf} which is as shown in Table 1. In the soil samples, χ_{fd} ranges from 0.07 to 22.07 with a mean of 2.227. The low values of χ_{fd} indicate that their magnetic properties are derived from coarse multi-domain (MD) or pseudo-single domain (PSD) grains⁽²²⁾. According to Bouhsane⁽¹⁸⁾, low χ_{fd} values likely indicate the formation of pedogenetic formation of magnetic particles in soils. The elevated values of χ_{fd} in some locations (TVM 50 & TVM 45), indicate that the soil samples are contaminated with magnetic minerals⁽⁴⁾. This could be due to anthropogenic emissions containing fine particles with a high magnetic nature that contaminate the soil.

According to Dearing⁽¹⁶⁾ semi-quantitative model, environmental magnetic samples can be classified into four categories: low FD (%) < 2.0% virtually no SP grains; Medium FD (%) 2.0– 10.0 % Admixture of SP and coarser non-SP grains or SP; High FD (%) 10.0 – 14.0% virtually all (> 75%) SP grains Very high FD (%) > 14 % which represent infrequent values, inexact measurements, or pollution. In soil samples the value of χ_{fd} % varied 0.07 to 22.07 with a mean of 2.227. The results of this work based on the above described semi-quantitative model indicates that the majority of samples (about 64%) contain virtually no SP grains, while the remaining 36% of samples contain an admixture of SP and coarser non-SP grains. The sample TVM 45 has a high percent FD value, indicating that virtually all (> 75%) SP grains are present, while TVM 50 has a percent FD value of 22.07, indicating that the soil samples are contaminated with magnetic minerals. The majority of the soil samples in the area have no SP grains, although a little may include SP and coarse MD magnetic grain. Figure 7 shows the % FD values with the locations.

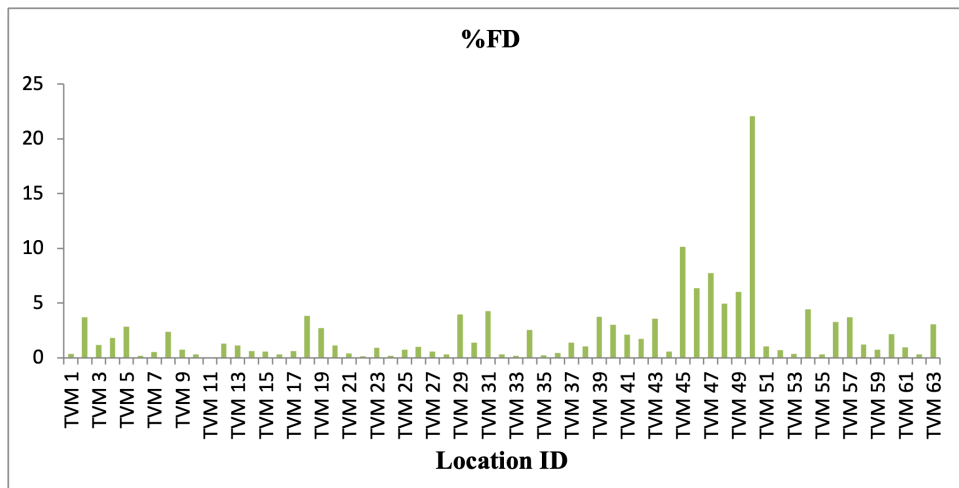


Fig 7. Location Vs Frequency dependent susceptibility (FD) %

3.6 Multivariate statistical analysis

3.6.1 Basic statistics

The statistical properties of the physicochemical and magnetic susceptibility were determined using basic statistics such as minimum, maximum, mean, standard deviation, variance, skewness, and kurtosis, as shown in Table 2. The degree of uniformity is low when the standard deviation exceeds the mean, and vice versa⁽²³⁾. In this present study, the standard deviation values of the analyzed parameters are higher than their mean value. This demonstrates that the low degree of uniformity⁽²⁴⁾. Skewness is a measure of the asymmetry of a real-valued random variable's probability distribution in probability theory and statistics. The degree of asymmetry of a distribution around its mean is measured by its skewness⁽²⁵⁾. A distribution with a positive skewness has an asymmetric tail that extends to greater positive values. A distribution with a negative skewness has an asymmetric tail that extends to negative values. Lower skewness levels imply that the distributions are more normal.

The positive value of the skewness of silt percent, clay percent, EC, pH, χ_{lf} , χ_{hf} and χ_{fd} in Table 2 indicates that the distributions are asymmetric in nature. The skewness of the sand percentage was negative; indicating an asymmetric distribution with an asymmetric tail extending toward more negative values. Kurtosis is a measure of the peakedness of a real-valued random variable's probability distribution. In comparison to the normal distribution, it describes the distribution's relative peakedness or flatness. It is referred to as mesokurtic, leptokurtic, or platykurtic depending on the peakedness. A normal curve, also known as a mesokurtic curve, has a kurtosis value of zero. When the kurtosis value is positive, the curve is more peaked than the normal curve, and when the kurtosis value is negative, the curve is less peaked than the normal curve, i.e., platykurtic⁽²⁶⁾. The positive kurtosis values of EC, χ_{lf} , χ_{hf} and χ_{fd} suggest that the curve is more peaked than the standard curve, indicating that it is leptokurtic. The percentage of sand, silt, clay, and pH kurtosis values are all negative, indicating a platykurtic distribution. This may be because the samples in the study area had an uneven distribution of such parameters. The frequency distributions of all the examined parameters that were analyzed are shown in Figures 8, 9, 10, 11, 12, 13, 14 and 15, along with histograms. The graphs for silt%, clay%, EC & pH normal (bell-shaped) distributions and magnetic susceptibility values of χ_{lf} , χ_{hf} and χ_{fd} exhibit some degree of multi-modality⁽²⁴⁾.

Table 2. Basic statistical data of the studied parameters

	Basic Statistics							
	Sand %	Slit %	Clay %	EC	pH	LF*	HF*	%FD
Mean	76.46	15.16	8.38	177.63	6.87	273.39	270.51	2.27
Median	77.00	15.00	9.00	123.80	6.75	133.89	130.24	1.12
Mode	80.00	12.00	10.00	120.00	6.06	23.25	82.34	0.29
Std. Deviation	8.36	4.99	3.73	155.30	0.75	343.33	341.23	3.24
Variance	69.93	24.91	13.95	24117.43	0.57	117878.13	116435.66	10.54
Skewness	-0.12	0.24	0.05	2.76	0.53	2.33	2.32	4.129
Kurtosis	-1.12	-0.98	-0.78	7.06	-0.62	5.75	5.72	22.56
Range	29.00	20.00	14.00	681.70	3.26	1641.65	1627.91	22
Minimum	61.00	7.00	2.00	61.30	5.50	23.25	20.09	0.07
Maximum	90.00	27.00	16.00	743.00	8.76	1664.90	1648.00	2.227
Sum	4817.00	955.00	528.00	11190.65	433.05	17223.32	17041.87	140.0

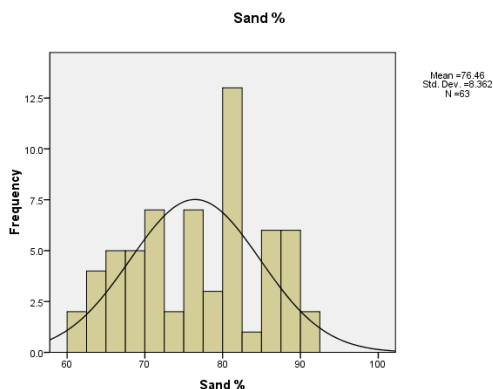


Fig 8. The frequency distribution of sand%

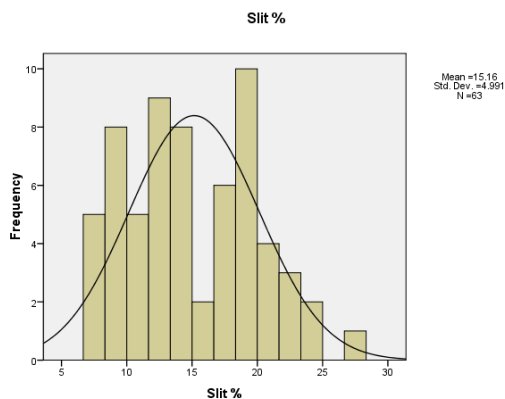


Fig 9. The frequency distribution of slit %

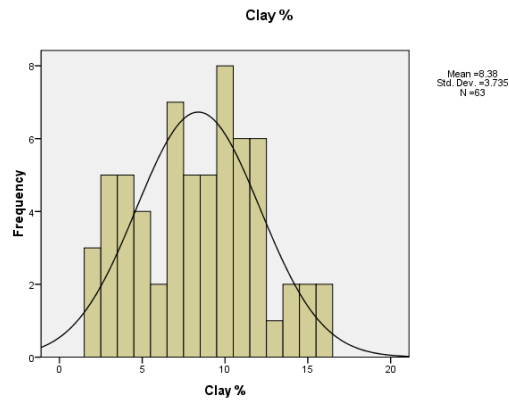


Fig 10. The frequency distribution of clay %

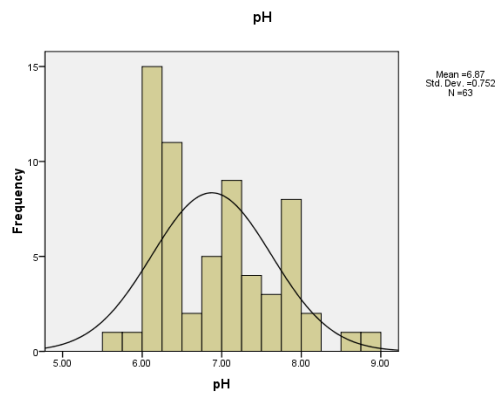


Fig 11. The frequency distribution of pH

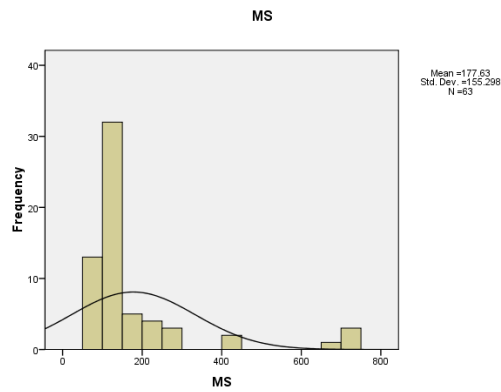


Fig 12. The frequency distribution of electrical conductivity

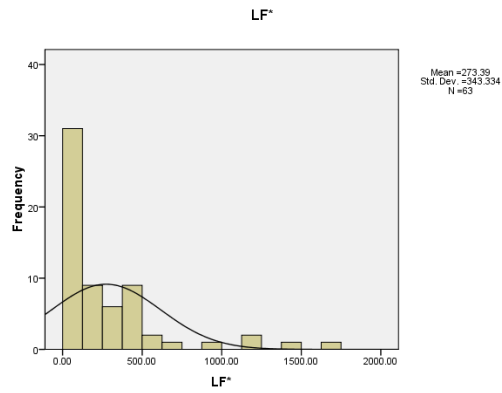


Fig 13. The frequency distribution of low frequency (LF)susceptibility

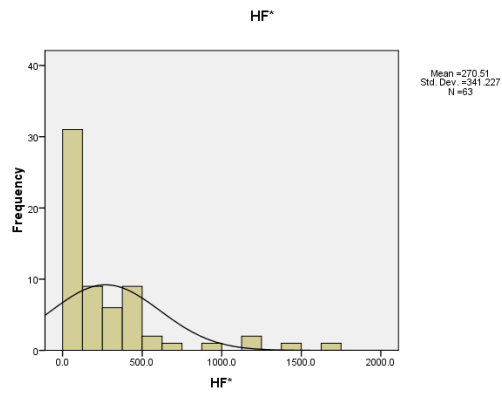


Fig 14. The frequency distribution of high frequency (HF) susceptibility

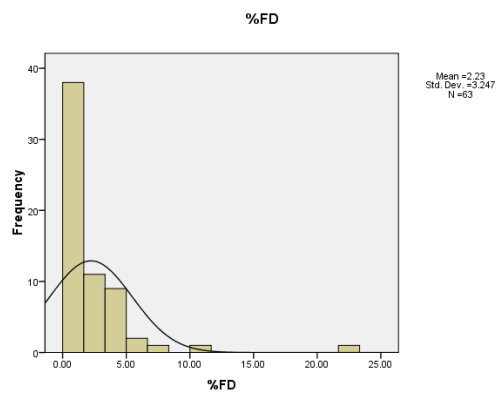


Fig 15. The frequency distribution of Fd%

3.7 Pearson correlation analysis

The Pearson correlation between physicochemical properties and magnetic susceptibility parameters in studied samples is reported in Table 3. As indicated by Table 3, there is a weak positive correlation between LF ($r=0.111$) and percent sand, while LF and HF have a weak negative correlation with percent silt, clay, EC, and pH. This means that sand content enhanced the level of magnetic minerals in the soil samples. A significant negative correlation ($r = 0.290$) exists between χ_{lf} and $\chi_{fd\%}$, indicating that χ_{lf} is strongly influenced by coarse-grained magnetic particles⁽²²⁾. The χ_{fd} has a negative correlation with the physicochemical parameters LF & HF, indicating that soils do not contain a significant amount of pedogenic magnetic particles. This finding indicates that the majority of pollution in urban soils is caused by anthropogenic inputs. Thus, correlations between magnetic parameters and physicochemical parameters in soils are likely to be influenced by the sources of magnetic particles and physicochemical parameters.

Table 3. Pearson correlation analysis physic chemical properties and magnetic susceptibilities

Variables	Sand %	Silt %	Clay %	EC	pH	LF*	HF*	%FD
Sand %	1							
Slit %	-0.969	1						
Clay %	-0.944	0.833	1					
EC	0.166	-0.159	-0.158	1				
pH	0.106	-0.078	-0.133	-0.111	1			
LF*	0.111	-0.123	-0.084	-0.045	-0.191	1		
HF*	0.111	-0.124	-0.084	-0.044	-0.191	1.000	1	
%FD	-0.050	0.101	-0.022	-0.108	0.335	-0.290	-0.293	1.000

3.8 Factor analysis (FA)

Factor analysis (FA) was used to explain the correlations between variables by extracting eigen values and eigen vectors from the covariance matrix of the original variables, lowering the data set’s dimensionality. The goal of this study is to find soil properties in a dataset that can explain a significant amount of the variance in the full population sampled using linear correlation. Varimax rotated factor variables for physicochemical properties and magnetic susceptibilities are shown in Table 4. As indicated in Table 4, factors I and II were extracted from the data set and explained approximately 78.5 percent of the overall variability. Factor I accounted for 26.65 percent of the variance, mainly due to high positive loadings of percent sand, LF, and HF, while Factor II accounted for 14.2 percent of the variance, mainly due to loadings of percent silt, clay, EC, pH, and percent FD. The findings of this study confirm the correlation analysis.

Table 4. Factor analysis of physico-chemical properties and magnetic susceptibilities

Variables	Factors	
	1	2
Sand %	0.093	0.182
Slit %	-0.105	-0.178
Clay %	-0.067	-0.171
EC	-0.150	0.989
pH	-0.177	-0.139
LF*	0.994	0.105
HF*	0.994	0.107
%FD	-0.277	-0.152
% of variance explained	26.65	14.20

3.9 Cluster analysis (CA)

The hierarchical approach proposed by⁽²⁷⁾ was used for Clustering. The properties were classified according to their degree of similarity in order to group them together in this analysis. The aim was to examine database similarity patterns and classify

them according to their dissimilarity coefficients. Euclidean distance is dimensionless and expresses similarity among diverse studied properties. This variable can be interpreted as a measure of the relationships that exist between groups of variables that have been analysed. The derived dendrogram is shown in Figures 16, 2 and 1. Cluster I was formed as a result of the percentages of sand, silt, clay, pH, EC, and %FD. Cluster II was formed as a result of LF and HF. This indicates that magnetic susceptibilities in soil samples are mostly determined by the amount of sand present. The clustering findings are supported by the factor analysis.

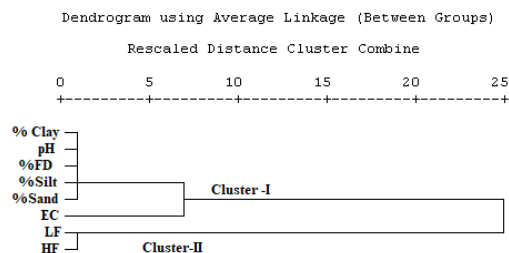


Fig 16. Dendrogram of cluster analysis

4 Conclusion

The results of magnetic susceptibility and Physico-chemical properties of soils in different areas of Tiruvannamalai district, Tamilnadu is presented in this study. According to the findings, the particle size was dominated by sand, followed by silt and then clay in samples and that 57 percent of samples are acidic in nature. The results of the percentage frequency dependence indicate that most of the samples have virtually no SP grains hence the observed magnetic susceptibility values result from a combination of pedogenic and anthropogenic sources. The amount of sand in the soil samples is highly associated with low and high frequency magnetic susceptibilities, according to statistical studies. It is concluded that magnetic measurements can be used as a proxy for detecting contamination levels and identifying pollution sources in soils. Magnetic measurements enable rapid and low-cost pollution measurements in urban areas.

References

- 1) Yu L, Oldfield F. A Multivariate Mixing Model for Identifying Sediment Source from Magnetic Measurements. *Quaternary Research*. 1989;32(2):168–181. Available from: [https://doi.org/10.1016/0033-5894\(89\)90073-2](https://doi.org/10.1016/0033-5894(89)90073-2). doi:[https://doi.org/10.1016/0033-5894\(89\)90073-2](https://doi.org/10.1016/0033-5894(89)90073-2).
- 2) Hanesch M, Scholger R. The influence of soil type on the magnetic susceptibility measured throughout soil profiles. *Geophysical Journal International*. 2005;161(1):50–56. Available from: <https://doi.org/10.1111/j.1365-246X.2005.02577.x>.
- 3) Valaee M, Ayoubi S, Khormali F, Lu SG, Karimzadeh HR. Using magnetic susceptibility to discriminate between soil moisture regimes in selected loess and loess-like soils in northern Iran. *Journal of Applied Geophysics*. 2016;127(2):23–30. Available from: <https://doi.org/10.1016/j.jappgeo.2016.02.006>.
- 4) Devanesan E, Chandrasekaran A, Sivakumar S, Joy KMF, Najam LA, Ravisankar R. Magnetic Susceptibility as Proxy for Heavy Metal Pollution Detection in Sediment. *Iranian Journal of Science and Technology, Transactions A: Science*. 2020;44(3):875–888. Available from: <https://doi.org/10.1007/s40995-020-00865-9>.
- 5) Hari Krishnan N, Chandrasekaran A, Ravisankar R, Alagarsamy R. Statistical assessment to magnetic susceptibility and heavy metal data for characterizing the coastal sediment of East coast of Tamilnadu, India. *Applied Radiation and Isotopes*. 2018;135:177–183. Available from: <https://doi.org/10.1016/j.apradiso.2018.01.030>.
- 6) Ravisankar R, Tholkappian M, Chandrasekaran A, Eswaran P, El-Taher A. Effects of physicochemical properties on heavy metal, magnetic susceptibility and natural radionuclides with statistical approach in the Chennai coastal sediment of east coast of Tamilnadu, India. *Applied Water Science*. 2019;9(7):151. Available from: <https://doi.org/10.1007/s13201-019-1031-8>.
- 7) Maher BA, Thompson R. Palaeomonsoons I: the magnetic record of palaeoclimate in the terrestrial loess and palaeosol sequences. In: *Quaternary Climates, Environments and Magnetism*; vol. 81. Cambridge University Press. 1999;p. 81–125.
- 8) Dearing JA. 1994.
- 9) Thompson R, Oldfield F, Magnetism. *London: Allen & Unwin*. 1986;p. 227–227.
- 10) Ganesh D, Eswaran P, Senthilkumar G, Bramha SN, Chandrasekaran S, Ravisankar R. A Quantitative Study of Natural Uranium Present in Groundwater of Tiruvannamalai District of India. *Iranian Journal of Science and Technology, Transactions A: Science*. 2021;45(2):545–555. Available from: <https://doi.org/10.1007/s40995-020-01011-1>.
- 11) Ganesh D, Senthilkumar G, Eswaran P, Balakrishnan M, Bramha SN, Chandrasekaran S, et al. A peep into the state of ground water quality in the district of Tiruvannamalai. *Applied Water Science*. 2021;11:83. Available from: <https://doi.org/10.1007/s13201-021-01411-7>.

- 12) Sonaye SY, Baxi RN. Particle size measurement and analysis of flour. *International Journal of Applied Engineering Research*. 2012;2:1839.
- 13) Shivanna AM, Nagendrappa G. Chemical Analysis of Soil Samples to Evaluate the Soil Fertility Status of Selected Command Areas of Three Tanks in Tiptur Taluk of Karnataka, India. *IOSR Journal of Applied Chemistry*. 2014;7(11):01–05. Available from: <https://doi.org/10.9790/5736-071110105>.
- 14) Zhang C, Qiao Q, Piper JDA, Huang B. Assessment of heavy metal pollution from a Fe-smelting plant in urban river sediments using environmental magnetic and geochemical methods. *Environmental Pollution*. 2011;159(10):3057–3070. Available from: <https://doi.org/10.1016/j.envpol.2011.04.006>.
- 15) Liu Q, Torrent J, Maher BA, Yu Y, Deng C, Zhu R, et al. Quantifying grain size distribution of pedogenic magnetic particles in Chinese loess and its significance for pedogenesis. *Journal of Geophysical Research: Solid Earth*. 2005;110(11):1–1. Available from: <https://doi.org/10.1029/2005JB003726>.
- 16) Dearing JA. Environmental Magnetic Susceptibility, Using the Bartington MS2 System. England. Chi Publishing, 1999.
- 17) Lal R, Shukla MK. Principles of Soil Physics. New York. CRC Press. 2004.
- 18) Bouhsane N, Bouhlassa S. Assessing Magnetic Susceptibility Profiles of Topsoils under Different Occupations. *International Journal of Geophysics*. 2018;2018:1–8. Available from: <https://doi.org/10.1155/2018/9481405>.
- 19) Maher BA. Characterisation of soils by mineral magnetic measurements. *Physics of the Earth and Planetary Interiors*. 1986;42(86):80010–80013. Available from: [https://doi.org/doi.org/10.1016/S0031-9201\(86\)80010-3](https://doi.org/doi.org/10.1016/S0031-9201(86)80010-3).
- 20) Sadiki A, Faleh A, Navas A, Bouhlassa S. Using magnetic susceptibility to assess soil degradation in the Eastern Rif, Morocco. *Earth Surface Processes and Landforms*. 2009;34(15):2057–2069. Available from: <https://doi.org/doi.org/10.1002/esp.1891>.
- 21) Maher BA. Magnetic properties of modern soils and Quaternary loessic paleosols: paleoclimatic implications. *Palaeogeography, Palaeoclimatology, Palaeoecology*. 1998;137(1-2):25–54. Available from: [https://doi.org/10.1016/S0031-0182\(97\)00103-X](https://doi.org/10.1016/S0031-0182(97)00103-X).
- 22) Zong Y, Xiao Q, Lu S. Magnetic signature and source identification of heavy metal contamination in urban soils of steel industrial city, Northeast China. *Journal of Soils and Sediments*. 2017;17(1):190–203. Available from: <https://doi.org/10.1007/s11368-016-1522-2>.
- 23) Ravisankar R, Sivakumar S, Chandrasekaran A, Jebakumar JPP, Vijayalakshmi I, Vijayagopal P, et al. Spatial distribution of gamma radioactivity levels and radiological hazard indices in the East Coastal sediments of Tamilnadu, India with statistical approach. *Radiation Physics and Chemistry*. 2014;103:89–98. Available from: <https://doi.org/10.1016/j.radphyschem.2014.05.037>.
- 24) Sivakumar S, Chandrasekaran A, Senthilkumar G, Gandhi MS, Ravisankar R. Determination of radioactivity levels and associated hazards of coastal sediment from south east coast of Tamil Nadu with statistical approach. *Iranian Journal of Science and Technology, Transactions A: Science*. 2018;42(2):601–614. Available from: <https://doi.org/10.1007/s40995-017-0184-2>.
- 25) Groeneveld RA, Meeden G. Measuring Skewness and Kurtosis. *The Statistician*. 1984;33(4):391–391. Available from: <https://doi.org/10.2307/2987742>.
- 26) Gupta SP. Statistical Methods. . 2001.
- 27) Sneath PH, Sokal RR. Numerical taxonomy: The principles and practice of numerical classification. vol. 573. San Francisco. W. H. Freeman. 1973. Available from: <https://doi.org/10.2307/2987742>.